ACS APPLIED MATERIALS & INTERFACES

Letter

www.acsami.org

Topographical Binding to Mucosa-Exposed Cancer Cells: Pollen-Mimetic Porous Microspheres with Tunable Pore Sizes

Jiantao Feng,[†,‡,§] Ling Lin,[†,⊥,#] Peipei Chen,[§] Wenda Hua,[§,∥] Quanmei Sun,[§] Zhuo Ao,[§] Dongsheng Liu,[‡] Lei Jiang,[#] Shutao Wang,*[,#] and Dong Han*[,§]

[‡]Key Laboratory of Organic Optoelectronics & Molecular Engineering of the Ministry of Education, Department of Chemistry, Tsinghua University, Beijing 100084, China

[⊥]Engineering Research Center of Marine Biological Resource Comprehensive Utilization, The Third Institute of Oceanography of the State Oceanic Administration, Xiamen 361005, China

[§]National Center for Nanoscience and Technology, Beijing 100190, China

[#]Beijing National Laboratory for Molecular Sciences (BNLMS), Key Laboratory of Organic Solids, Institute of Chemistry, Chinese Academy of Sciences, Beijing 100190, China

[∥]First Affiliated Hospital of Kunming Medical University, Kunming 650032, China

Supporting Information

ABSTRACT: Mucoadhesives have been perceived as an effective approach for targeting the mucosa-associated diseases, which relied on the adhesive molecules to enhance the specificity. Here, topographical binding is proposed based on the fabrication of surface pore size tunable pollen-mimetic microspheres with phase separation and electrospray technology. We proved that microspheres with large-pores (pore size of 1005 ± 448 nm) were the excellent potential candidate for the mucoadhesives, as they not only possessed better adhesion ability, but also could topographically bind cervical cancer cells. Our methods of topographical binding offered a new way of designing the mucoadhesives for treating the mucosa-associated diseases.

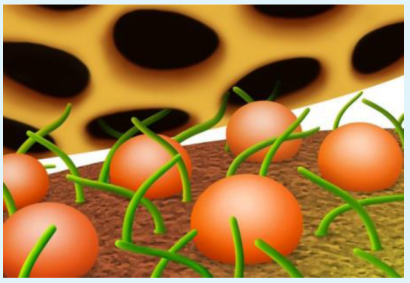

KEYWORDS: *microsphere, adhesive, topographical binding, mucosa, cancer cell*

INTRODUCTION

Mucoadhesives have been focused recently on the field of mucosa-associated diseases as a complementary approach instead of intravenous injection for building a novel system of drug delivery or vaccine carrier,[1,2] because of their advantages of prolonging the residence time at the site of drug absorption, small dosage, better specificity, and reduced side effects compared to the traditional drugs.[2−4] For cancer treatments, especially in the respiratory system, oral cavity, gastrointestinal tract, and vagina, tumors exist together with normal epithelial tissues, always exposing in the mucosal membrane.[5] Hence it is particularly crucial to target tumor cells and transport drugs into the cells via mucosa administration. Presently different approaches of making mucoadhesives have been extensively studied for enhancing the adhesion efficiency. Chemical approaches were applied to produce kinds of polymeric bioadhesive platforms such as hydrophilic polymers, hydrogels, co-polymers/interpolymer complex, and thiomers.[3,6] On the other hand, microfabrication techniques were introduced to design precisely shaped structures, such as microneedles and microposts, which could increase the adhesive elements per surface area.[7−9] Additionally, for strengthening the bind with the targeted organ or tissue, more specific systems were designed based on lectin, thiol, and various other adhesive functional groups.[10−12] However, all the methods mentioned above have to employ adhesive molecules to enhance the specificity, which increased the cost of the product and complicated the fabrication process as a result.

Here, we explored a new method for fabricating the potential mucoadhesives to topographically bind the cancer cells without the modification of special molecules. In this paper, inspired by pollen microstructures, phase separation was introduced into the process of electrospray and tunable pore sizes from nanoscales to microscales on surface of microspheres were prepared by modifying the volume ratio of the non-solvent in electrospray solution. Adhesion ability of the microspheres was measured with CasKi cells (cervical cancer cell line) and Ect1/E6E7 cells (cervical epithelial cell line). Atomic force microscope (AFM) was employed to analyze the adhesion between cells and pollen-mimetic microspheres, which were attached on the tipless AFM cantilevers.

MATERIALS AND METHODS

1. Fabrication of Pollen-Mimetic Microspheres. Polycaprolactone (PCL) (M_w 65000, Sigma) was dissolved at a

Received: March 20, 2014
Accepted: May 12, 2014
Published: May 12, 2014

DOI: 10.1021/am5016827
ACS Appl. Mater. Interfaces 2015, 7, 8961−8967

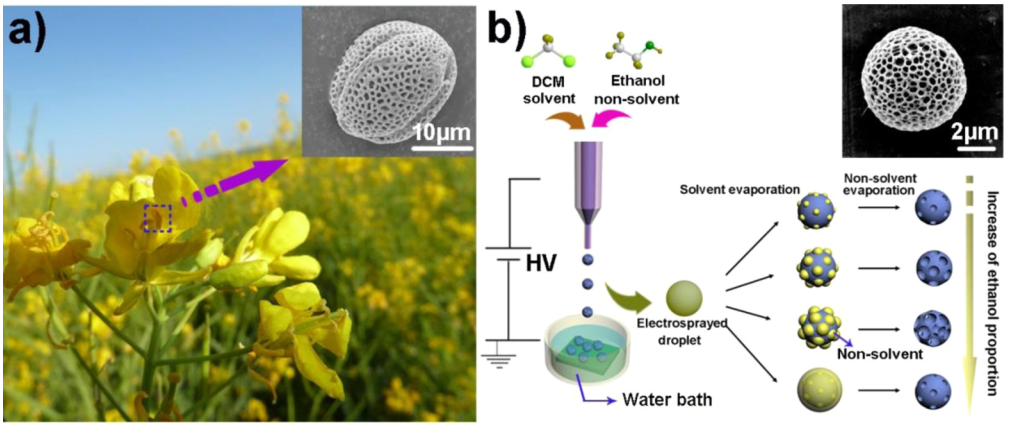

Figure 1. Fabrication of pollen-mimetic microspheres. (a) Canola flower and low-vacuum scanning electron microscope (SEM) imaging of the pollens. (b) Illustration of microspheres generation with different pore sizes on surface by changing nonsolvent ratios. In step one, solvent (DCM) quickly evaporated before microspheres arriving at the collector. In step two, nonsolvent (ethanol) evaporated slowly and porous microstructures formed at surface of the particles in a water bath. Insert figure shows a representative SEM picture of the pollen-mimetic microspheres.

concentration of 3% (wt %) in ethanol and dichloromethane (DCM) mixture at following ratios (v/v): 0, 1/60, 1/30, and 1/15. During the electrospray process, the polymer solution was fed at 3 mL h^{-1} using a syringe needle (inner diameter of 0.17 mm) under a voltage of 15 kV, while keeping the temperature and humidity at 25 °C and 30%. The distance between the tip of the needle and the collector was fixed at 20 cm. Microspheres were collected in a water bath.

2. Cell Culture and Adhesion Measurement. Cervical cancer cell line CasKi (ATCC, CRM-CRL-1550) was maintained in RPMI1640 medium supplemented with 10% fetal bovine serum (FBS), 100 U ml^{-1} penicillin and 100 mg mL^{-1} streptomycin (all from Hyclone). Cervical epithelial cell line Ect1/E6E7 (ATCC, CRL-2614) was cultured in Keratinocyte medium containing 0.1 ng mL^{-1} human recombinant EGF and 0.05 mg mL^{-1} bovine pituitary extract (all from Gibco).

For adhesion measurements, tipless AFM cantilever (NTMDT, CSG11/tipless) was attached with microspheres by UV-sensitive glue. CasKi and Ect1/E6E7 cells were transferred in a petri dish and allowed to proliferate for 48 h. Afterwards, dishes were placed on sample stage of AFM system (Agilent, 5500) which combines an inverted microscope (Nikon, TE2000U). Each cell was probed with above cantilevers to record force−distance curves at the central position of the cytoplasm with a frequency of 10 Hz.

3. Low-Vacuum Scanning Electron Microscope (SEM) Characterizations. After fixation in 2.5% (w/w %) glutaraldehyde for 3 h, cell samples were dehydrated through graded ethanol solutions of 30, 50, 70, 85, 95, and 100%, for 10 min each. The samples were then dried by a critical point dryer (Balzers CPD 030) and imaged by scanning electron microscope (Quanta 200) under low-vacuum mode. Pollens were imagined followed an ultrasonic cleaning in ethanol and acetone, respectively. The microspheres could be directly observed without any pretreatment by the low-vacuum SEM.

RESULTS AND DISCUSSION

In nature, the mucous membrane in the respiratory tract can be easily adhered by pollen grains assisted by the reticulate ultrastructures,[13,14] as shown on pollens of the canola flower (Figure 1a), which could be modeled as the microspheres with the porous topography on surface. Hence, the specific topography of the pollens can be imitated to design drug carriers that bind the mucosa. Variant methods fabricating microspheres or pore structures have been extensively investigated, such as membrane emulsification technique,[15,16] phase separation,[17] self-assembly,[18] breath figure technique,[19,20] and spray pyrolysis.[21−23] Among these methods, electrospinning has been chosen as a versatile platform to produce the fibers and microspheres with some specific secondary structures, e.g., core/sheath, hollow, and porous.[24−28] As a special case of electrospinning, electrospraying shares similar physical principles and can be applied to fabricate the particles at mico/nanoscales.[29,30] Although microspheres with porous structures have been reported employing the electrospray or spray-drying technique,[31−34] the size-controllable porous structures on surface have not been achieved yet. For generating the microspheres with tunable pore sizes on surface, we added ethanol in small proportions into the polycaprolactone (PCL) solution as the nonsolvent.

Biodegradable PCL was used in this study as having similar surface energy with carotenoid, which is a critical constituent in the outer pollen.[35] PCL was dissolved in dichloromethane (DCM) at a concentration of 3% (wt %), with different low proportions of ethanol as the nonsolvent. During the electrospray process, the polymer solutions were loaded in a syringe that was connected to the high-voltage power, developing a conical shape called Taylor cone at tip of the nozzle. When the electrostatic forces overcame the limit of surface tension, polymer solution was ejected from the Taylor cone and microspheres of different sizes formed following the evaporation and stretching processes in electric field.[30] In our experiment, solvent (DCM) and nonsolvent (ethanol) had different vapor pressures (DCM: 46.59 kPa/20°C, ethanol: 5.67 kPa/20°C), which resulted in the evaporation in different steps during phase separation. As shown in Figure 1b, the formation of the porous microspheres can be divided into two steps. In the first step, solvent (DCM) quickly evaporated before microspheres arrived at the collector, leaving nonsolvent ethanol distributed on the surface of PCL particles, whereas in the second step, nonsolvent (ethanol) evaporated slowly and porous microstructures formed at surface of the particles in a water bath. The generation of the porous structures was accomplished by phase separation, which was induced by increasing temperature and evaporation.[36] After phase separa-

DOI: 10.1021/am5016827
ACS Appl. Mater. Interfaces 2015, 7, 8961−8967

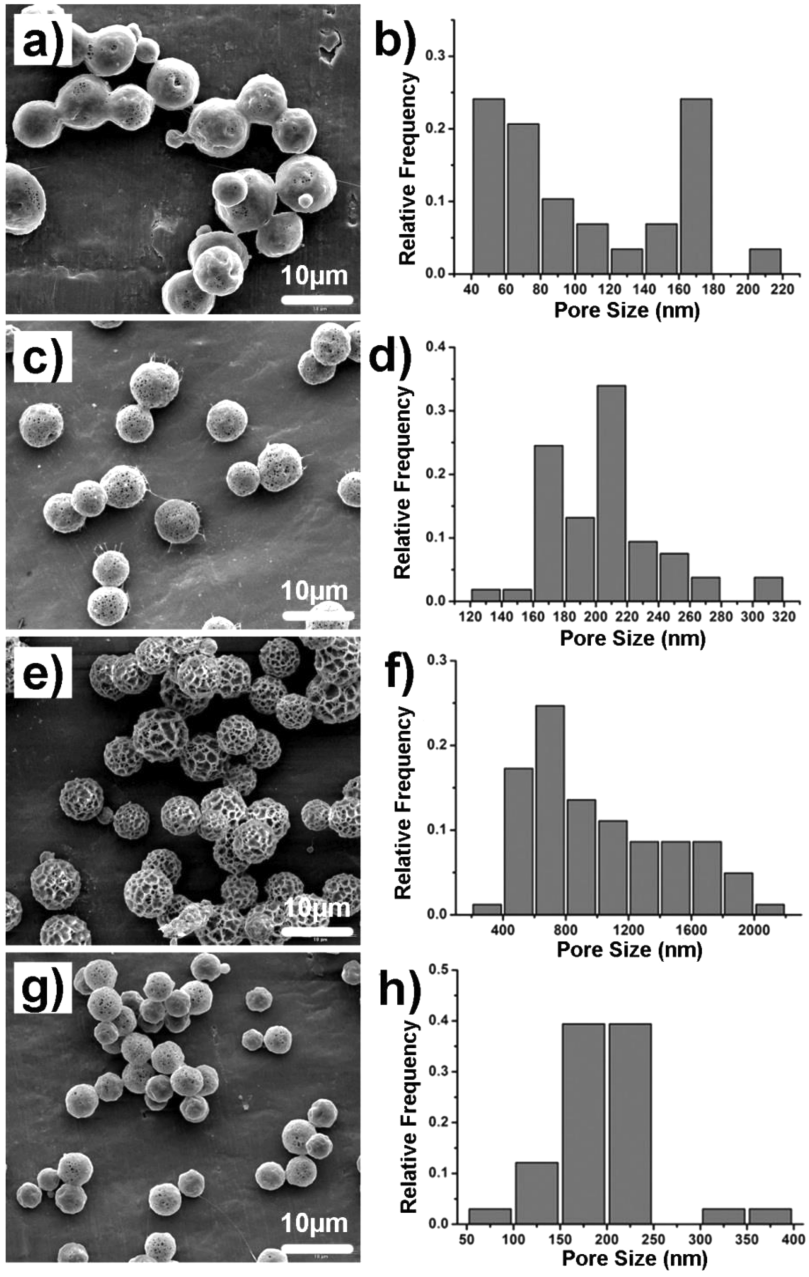

Figure 2. Low-vacuum SEM imaging of microspheres with different pore sizes after changing ethanol ratios (v/v) from (a, b) 0 to (c, d) 1/60, (e, f) 1/30, and (g, h) 1/15. Average pore sizes on microspheres were generated as (b) 108 ± 48 nm, (d) 206 ± 37 nm, (f) 1005 ± 448 nm, and (h) 191 ± 54 nm, respectively.

tion, the concentrated polymer phase solidified shortly and formed the particle matrix, whereas the polymer poor phase formed the pores.[34]

As shown in Figure 2, different pore sizes on microspheres were prepared by adjusting the ethanol ratios in electrospray solution. Here, 50−60 microspheres from different batches were randomly selected for the size measurements. When ethanol ratios (v/v) changed from 0 to 1/60, 1/30, and 1/15, average pore sizes on microspheres were generated as 108 ± 48 nm (Figure 2a, b), 206 ± 37 nm (Figure 2c, d), 1005 ± 448 nm (Figure 2e, f), and 191 ± 54 nm (Figure 2g, h) respectively. Diameters of microspheres (6.14 ± 0.59 μm) in the above groups did not change significantly as the same PCL concentration was shared. Consequently, with the increase in proportion, ethanol gathered on the surface of the particles in larger clusters and densities, forming pores with increasing diameter. However, pore size decreased when ethanol volume ratio exceeded 1/30 (v/v), which may be caused by the overall covering of ethanol on surface of the particles and offering no contribution for pore generation (Figure 1b). The porous structures with some degree of tortuosity mainly distributed on surface of the particles, indicating that the process of phase separation occurred on the surface of the microspheres (see the Supporting Information, Figure S1). According to above principles, similar pollen-mimetic particles were also prepared by changing ethanol as acetic acid (see the Supporting Information, Figure S2), further demonstrating the wide feasibility of our method.

The pollen-mimetic microspheres can find their applications in fields of controlled release systems, tissue engineering and

DOI: 10.1021/am5016827
ACS Appl. Mater. Interfaces 2015, 7, 8961−8967

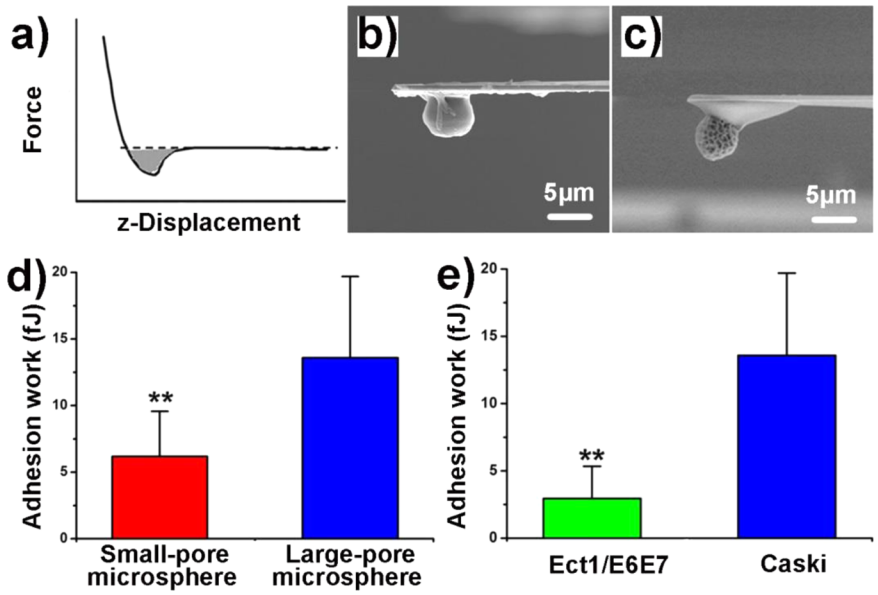

Figure 3. Adhesion energy measurements with the atomic force microscope (AFM) cantilever on CasKi cells and Ect1/E6E7 cells. (a) Retracting part of a typical force curve. The shallow area represents adhesion energy. (b) Tipless AFM cantilever attached with small-pore microsphere (pore size of 108 ± 48 nm). (c) Tipless AFM cantilever attached with large-pore microsphere (pore size of 1005 ± 448 nm). (d) Adhesion energy of large-pore microsphere on CasKi cells (13.58 ± 6.12 fJ) was significantly larger than the value of small-pore microsphere (6.18 ± 3.39 fJ) ($p < 0.001$), indicating that microspheres with a large pore size (1005 ± 448 nm) are more suitable as the drug carriers. (e) Adhesion energy of large-pore microsphere on CasKi cells (13.58 ± 6.12 fJ) was five times larger than the value on Ect1/E6E7 cells (2.95 ± 2.4 fJ), indicating a good specificity of the topographical binding.

cosmetics, et al.,[37,38] in which adhesion capability plays a critical role in evaluating the practicability. Several theories have been adapted for the investigation of adhesion, among which the fracture theory relates the adhesive strength to the forces required for detachment of the two involved surfaces after adhesion.[39] According to the theory, atomic force microscope (AFM) was applied to detect the adhesion energy (γ) at single microsphere level, which was calculated by the integral of the force−distance attractive force[40]

$$\gamma = \int F(z)dz \tag{1}$$

where γ represents the shallow area in Figure 3a, F is the adhesive force when the AFM probe is retracted away from the substrate, and z is the relative distance of the cantilever holder to the surface.

We next measured the adhesion energy between pollen-mimetic microspheres and mucosa-exposed cancer cells. The cervix is classified as a fully exposed organ of the human body. Cervical cancer originated in cervical mucosa and tumor cells mainly spread over the suprabasal differentiating cell layers of the cervical epithelial dysplasia, thus offering a target for the adhesive drug carriers.[41,42] Hence cervical cancer cells were used as the model to test the function of the pollen-mimetic microspheres as a universally applicable mucoadhesives. To investigate the influence of pore size on adhesion, we attached tipless AFM cantilevers with the small-pore (108 ± 48 nm) microsphere (Figure 3b), and large-pore (1005 ± 448 nm) microsphere (Figure 3c), respectively. The former cantilever was detected with a spring constant (K) of 0.647 N m^{-1} and a sensitivity (S) of 8.806 nm V^{-1} and the other was detected with a K of 0.502 N m^{-1} and an S of 10.669 nm V^{-1}. Cervical cancer cell line CasKi, established from human cervical carcinomas,[43] was used for adhesion analysis of the microspheres. Both of the cantilevers were applied to collect AFM force curves of CasKi cells with a frequency of 10 Hz. To compare the adhesion of microspheres, we detected more than 40 CasKi cells. Results showed that the average adhesion energy of small-pore microsphere and large-pore microsphere were 6.18 ± 3.39 fJ and 13.58 ± 6.12 fJ respectively (Figure 3d). The difference was significant by performing Student's t-Test ($p < 0.0001$). Besides, we also find that adhesion force of large-pore microsphere on Caski cells was significantly larger than the value of small-pore microsphere (see the Supporting Information, Figure S3). The interesting result that different pore sizes lead to varied adhesive condition between pollen-mimetic microspheres and cancer cells suggested that mucosa-exposed cancer cells could be topographically bound through the size tunable surface ultrastructure.

According to above results, the microspheres with size-tunable porous structures could be used as potential adhesives that carrying antitumor drugs in order to kill cervical cancer cells. Because the side effects of chemotherapy on normal cells have been widely focused,[44] we further analyzed the adhesion energy between large-pore microsphere and normal cervical epithelial cells, for example, the ectocervical Ect1/E6E7 cell line, which was established from normal epithelial tissue taken from a premenopausal woman undergoing hysterectomy for endometriosis.[45] AFM cantilever attached with large-pore (1005 ± 448 nm) microsphere was used to collect force curves on more than 40 Ect1/E6E7 cells. The calculated average adhesion energy was 2.95 ± 2.4 fJ, which was only one-fifth of the adhesion energy on CasKi cells (13.58 ± 6.12 fJ). Difference was significant by performing Wilcoxon Two-Sample Test ($p < 0.0001$) (Figure 3e). We also find that adhesion force of large-pore microsphere on Caski cells was significantly larger than the value on Ect1/E6E7 cells (see the Supporting Information, Figure S4). The data indicated that the microspheres with pore size of 1005 ± 448 nm have a stronger adhesion on cervical cancer cells than that on normal cells,

DOI: 10.1021/am5016827
ACS Appl. Mater. Interfaces 2015, 7, 8961−8967

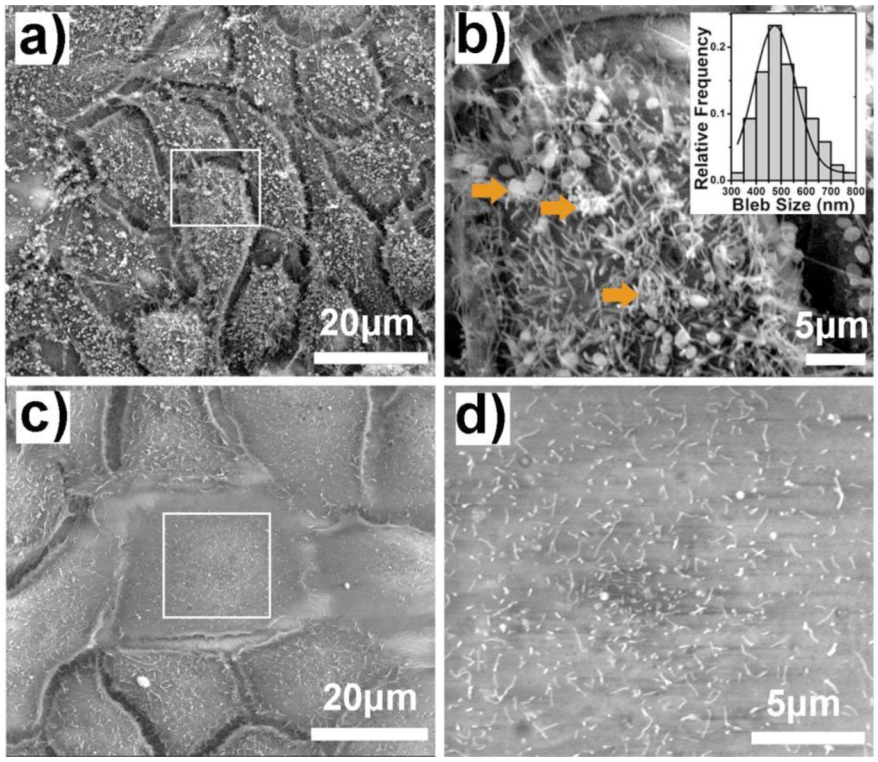

Figure 4. SEM imaging of (a) CasKi cells and (c) Ect1/E6E7 cells. (b, d) Enlargement of the corresponding squares in a and c. The membrane of CasKi cells was characterized by long microvilli and considerable protuberance like blebs with a diameter of 510.57 ± 93.96 nm. The adjacent microvilli interlaced around a protuberance, shaping an island-like structure (yellow arrow). No blebs were found on the surface of Ect1/E6E7 cells and only little short microvilli randomly appeared.

further confirming the good specificity of the topographical binding.

To explore what factor decided the adhesion events between different types of cells and the microspheres, we applied scanning electron microscopy for demonstrating the topographical differences in CasKi and Ect1/E6E7 cells. After fixation, dehydration and critical point drying, CasKi and Ect1/E6E7 cells were imagined in a low vacuum scanning electron microscope, which making sure that the high-resolution images of original conditions of cells could be achieved without prespinning Au. Results showed that the membrane of CasKi cells was characterized by long microvilli and considerable protuberances like blebs with a diameter of 511 ± 94 nm (Figure 4a, b). Furthermore, the adjacent microvilli interlaced around a nanoscaled bleb, shaping an islandlike structure (see arrows in Figure 4b). However, no blebs were found on the surface of Ect1/E6E7 cells and only little short microvilli randomly appeared (Figure 4c, d). The phenomenon was consistent with in situ observations. The ultrastructure of normal epithelial cells' luminal surface display more different profiles in comparison with that of cervical cancer cells.[46] There is a clearly evident that the microspheres with rational-sized pores may better match the irregularly distributed islandlike structures on cancer cells rather than normal cells. In our case, the porous microspheres with pore size of 1005 ± 448 nm lead to a topographical interaction with CasKi cells resulting in the specific adhesion. Furthermore, topographic changes of cell surface ultrastructure also extensively presented in other mucosa-associated tumors, such as colon cancer and gastric cancer,[47,48] indicating that the principle of topographical adhesion can also be applied to design drug carrying systems binding other mucosa.

CONCLUSIONS

In summary, we realized the topographical binding to the cervical cancer cells via the fabrication of surface pore size tunable pollen-mimetic microspheres with phase separation and electrospray technology. By changing the nonsolvent ratios in electrospray solution, different pore sizes from nanoscales to microscales could be generated on surface of the microspheres. We further confirmed that large-pore microspheres were the excellent potential candidate for the mucoadhesives of cervical cancer mucosa, as they not only possessed better adhesion ability than small-pore microspheres, but also could topographically bind the cervical cancer cells. The correlation between the structure and the function has been a fundamental principal in biological system from molecular level to the cell and tissue level.[49] Here, the specific ultrastructure induced topographical adhesion was called "topography coupled mechanical biofunction". Consequently, when designing adhesion-controlled materials, both the topographical characteristic of biological samples and the materials should be considered equally for enhancing the adhesion and related specificity. Also, the phase separation and electrospray combined method has a wide feasibility for producing surface pore tunable microspheres by altering the volume ratios of solvent and nonsolvent. Further, the pollen-inspired microspheres can be applied not only in the treatment of cervical cancer but also in other mucosa-associated diseases in the respiratory system, oral cavity, gastrointestinal tract, etc.

DOI: 10.1021/am5016827
ACS Appl. Mater. Interfaces 2015, 7, 8961−8967

■ ASSOCIATED CONTENT

Supporting Information

Pollen-mimetic particles were prepared by changing ethanol as acetic acid. This material is available free of charge via the Internet at http://pubs.acs.org/.

■ AUTHOR INFORMATION

Corresponding Authors

*E-mail: dhan@nanoctr.cn.
*E-mail: stwang@iccas.ac.cn.

Author Contributions

†Authors J.F. and L.L. contributed equally. The manuscript was written through contributions of all authors. All authors have given approval to the final version of the manuscript.

Notes

The authors declare no competing financial interest.

■ ACKNOWLEDGMENTS

This work was supported by the project of 973 in Ministry of Science and Technology of China (Grant 2012CB9333800), the National Natural Science Foundation of China (21301036), and the Key Research Program of the Chinese Academy of Sciences (KJZD-EW-M01).

■ ABBREVIATIONS

PCL, polycaprolactone
DCM, dichloromethane
AFM, atomic force microscope

■ REFERENCES

(1) Yoo, J.W.; Irvine, D. J.; Discher, D. E.; Mitragotri, S. Bio-inspired, Bioengineered and Biomimetic Drug Delivery Carriers. *Nat. Rev. Drug Discovery* **2011**, *10*, 521−535.

(2) Rosen, H.; Abribat, T. The Rise and Rise of Drug Delivery. *Nat. Rev. Drug Discovery* **2005**, *4*, 381−385.

(3) Roy, S.; Prabhakar, B. Bioadhesive Polymeric Platforms for Transmucosal Drug Delivery Systems−a Review. *Trop. J. Pharm. Res.* **2010**, *9*, 91−104.

(4) Singh, I.; Rana, V. Enhancement of Mucoadhesive Property of Polymers for Drug Delivery Applications. *Rev. Adhes. Adhes.* **2013**, *1*, 271−290.

(5) O'Hagan, D. T. Microparticles and Polymers for the Mucosal Delivery of Vaccines. *Adv. Drug Delivery Rev.* **1998**, *34*, 305−320.

(6) Nagai, T. Topical Mucosal Adhesive Dosage Forms. *Med. Res. Rev.* **1986**, *6*, 227−242.

(7) Sant, S.; Tao, S. L.; Fisher, O. Z.; Xu, Q. B.; Peppas, N. A.; Khademhosseini, A. Microfabrication Technologies for Oral Drug Delivery. *Adv. Drug Delivery Rev.* **2012**, *64*, 496−507.

(8) Fischer, K. E.; Alemán, B. J.; Tao, S. L.; Daniels, R. H.; Li, E. M.; Bünger, M. D.; Nagaraj, G.; Singh, P.; Zettl, A.; Desai, T. A. Biomimetic Nanowire Coatings for Next Generation Adhesive Drug Delivery Systems. *Nano Lett.* **2009**, *9*, 716−720.

(9) Fischer, K. E.; Nagaraj, G.; Hugh Daniels, R.; Li, E.; Cowles, V. E.; Miller, J. L.; Bunger, M. D.; Desai, T. A. Hierarchical Nanoengineered Surfaces for Enhanced Cytoadhesion and Drug Delivery. *Biomaterials* **2011**, *32*, 3499−3506.

(10) Andrews, G. P.; Laverty, T. P.; Jones, D. S. Mucoadhesive Polymeric Platforms for Controlled Drug Delivery. *Eur. J. Pharm. Biopharm.* **2009**, *71*, 505−518.

(11) Park, J. H.; Saravanakumar, G.; Kim, K.; Kwon, I. C. Targeted Delivery of Low Molecular Drugs Using Chitosan and its Derivatives. *Adv. Drug Delivery Rev.* **2010**, *62*, 28−41.

(12) Shin, G. H.; Chung, S. K.; Kim, J. T.; Joung, H. J.; Park, H. J. Preparation of Chitosan-Coated Nanoliposomes for Improving the Mucoadhesive Property of Curcumin Using the Ethanol Injection Method. *J. Agric. Food Chem.* **2013**, *61*, 11119−11126.

(13) Pehlivan, S.; Özler, H. Pollen Morphology of Some Species of *Muscari* Miller (Liliaceae-Hyacinthaceae) from Turkey. *Flora* **2003**, *198*, 200−210.

(14) Sagun, V. G.; Levin, G. A.; van der Ham, R. W. Pollen Morphology and Ultrastructure of *Acalypha* (Euphorbiaceae). *Rev. Palaeobot. Palynol.* **2006**, *140*, 123−143.

(15) Ma, G. H.; Sone, H.; Omi, S. Preparation of Uniform-sized Polystyrene-polyacrylamide Composite Microspheres from a W/O/W Emulsion by Membrane Emulsification Technique and Subsequent Suspension Polymerization. *Macromolecules* **2004**, *37*, 2954−2964.

(16) Ma, G. H.; Nagai, M.; Omi, S. Study on Preparation and Morphology of Uniform Artificial Polystyrene−poly (methyl methacrylate) Composite Microspheres by Employing the SPG (Shirasu porous glass) Membrane Emulsification Technique. *J. Colloid Interface Sci.* **1999**, *214*, 264−282.

(17) Matsuyama, H.; Teramoto, M.; Nakatani, R.; Maki, T. Membrane Formation via Phase Separation Induced by Penetration of Nonsolvent from Vapor Phase. I. Phase Diagram and Mass Transfer Process. *J. Appl. Polym. Sci.* **1999**, *74*, 159−170.

(18) Dinsmore, A.; Hsu, M. F.; Nikolaides, M.; Marquez, M.; Bausch, A.; Weitz, D. Colloidosomes: Selectively Permeable Capsules Composed of Colloidal Particles. *Science* **2002**, *298*, 1006−1009.

(19) Connal, L. A.; Qiao, G. G. Honeycomb Coated Particles: Porous Doughnuts, Golf Balls and Hollow Porous Pockets. *Soft Matter* **2007**, *3*, 837−839.

(20) Srinivasarao, M.; Collings, D.; Philips, A.; Patel, S. Three-dimensionally Ordered Array of Air Bubbles in a Polymer Film. *Science* **2001**, *292*, 79−83.

(21) Okuyama, K.; Wuled Lenggoro, I. Preparation of Nanoparticles via Spray Route. *Chem. Eng. Sci.* **2003**, *58*, 537−547.

(22) Sumaiya, Z.; Chuah, A. L.; Koay, G.; Salmiah, A.; Choong, T. Effect of Solvent Concentration and Cooling Modes on Morphology, Particle Size Distribution, and Yield of Dihydroxystearic acid (DHSA) Crystals. *Part. Sci. Technol.* **2010**, *28*, 236−246.

(23) Fan, J. B.; Huang, C.; Jiang, L.; Wang, S. Nanoporous Microspheres: from Controllable Synthesis to Healthcare Applications. *J. Mater. Chem. B* **2013**, *1*, 2222−2235.

(24) Li, D.; Xia, Y. Electrospinning of Nanofibers: Reinventing the Wheel? *Adv. Mater.* **2004**, *16*, 1151−1170.

(25) McCann, J. T.; Marquez, M.; Xia, Y. Highly Porous Fibers by Electrospinning into a Cryogenic Liquid. *J. Am. Chem. Soc.* **2006**, *128*, 1436−1437.

(26) Zheng, J.; He, A.; Li, J.; Xu, J.; Han, C. C. Studies on the Controlled Morphology and Wettability of Polystyrene Surfaces by Electrospinning or Electrospraying. *Polymer* **2006**, *47*, 7095−7102.

(27) Abbasipour, M.; Khajavi, R. Nanofiber Bundles and Yarns Production by Electrospinning: A Review. *Adv. Polym. Technol.* **2013**, *32* (21363), 1−21363.9.

(28) Feng, J.; Wang, F.; Han, X.; Ao, Z.; Sun, Q.; Hua, W.; Chen, P.; Jing, T.; Li, H.; Han, D. Green Pathway" Different from Simple Diffusion in Soft Matter: Fast Molecule Transport within Micro/nanoscaled Multiphase Porous System. *Nano Res.* **2014**, *7*, 434−442.

(29) Zhang, Q.; Liu, J.; Wang, X.; Li, M.; Yang, J. Controlling Internal Nanostructures of Porous Microspheres Prepared via Electrospraying. *Colloid Polym. Sci.* **2010**, *288*, 1385−1391.

(30) Loscertales, I. G.; Barrero, A.; Guerrero, I.; Cortijo, R.; Marquez, M.; Gañán-Calvo, A. M. Micro/Nano Encapsulation via Electrified Coaxial Liquid Jets. *Science* **2002**, *295*, 1695−1698.

(31) Edwards, D. A.; Hanes, J.; Caponetti, G.; Hrkach, J.; Ben-Jebria, A.; Eskew, M. L.; Mintzes, J.; Deaver, D.; Lotan, N.; Langer, R. Large Porous Particles for Pulmonary Drug Delivery. *Science* **1997**, *276*, 1868−1872.

(32) Zhou, X.; Zhang, S.; Huebner, W.; Ownby, P.; Gu, H. Effect of the Solvent on the Particle Morphology of Spray Dried PMMA. *J. Mater. Sci.* **2001**, *36*, 3759−3768.

DOI: 10.1021/am5016827
ACS Appl. Mater. Interfaces 2015, 7, 8961−8967

(33) He, J.-H.; Liu, Y.; Xu, L.; Yu, J. Y. Micro Sphere with Nanoporosity by Electrospinning. *Chaos, Solitons Fractals* **2007**, *32*, 1096−1100.
(34) Wu, Y.; Clark, R. L. Controllable Porous Polymer Particles Generated by Electrospraying. *J. Colloid Interface Sci.* **2007**, *310*, 529−535.
(35) Paunov, V. N.; Mackenzie, G.; Stoyanov, S. D. Sporopollenin Micro-reactors for in-situ Preparation, Encapsulation and Targeted Delivery of Active Components. *J. Mater. Chem.* **2007**, *17*, 609−612.
(36) Megelski, S.; Stephens, J. S.; Chase, D. B.; Rabolt, J. F. Micro- and Nanostructured Surface Morphology on Electrospun Polymer Fibers. *Macromolecules* **2002**, *35*, 8456−8466.
(37) Anderson, J. M.; Shive, M. S. Biodegradation and Biocompatibility of PLA and PLGA Microspheres. *Adv. Drug Delivery Rev.* **2012**, *64* (Supplement), 72−82.
(38) Guo, C.-W.; Cao, Y.; Xie, S.-H.; Dai, W.-L.; Fan, K.-N. Fabrication of Mesoporous Core-Shell Structured Titania Microspheres with Hollow Interiors. *Chem. Commun.* **2003**, *6*, 700−701.
(39) Smart, J. D. The Basics and Underlying Mechanisms of Mucoadhesion. *Adv. Drug Delivery Rev.* **2005**, *57*, 1556−1568.
(40) Carpick, R. W.; Ogletree, D. F.; Salmeron, M. A General Equation for Fitting Contact Area and Friction vs Load Measurements. *J. Colloid Interface. Sci.* **1999**, *211*, 395−400.
(41) Schiffman, M.; Castle, P. E.; Jeronimo, J.; Rodriguez, A. C.; Wacholder, S. Human Papillomavirus and Cervical Cancer. *Lancet* **2007**, *370*, 890−907.
(42) Zur Hausen, H. Papillomaviruses and Cancer: from Basic Studies to Clinical Application. *Nat. Rev. Cancer* **2002**, *2*, 342−350.
(43) Lin, K.-Y.; Guarnieri, F. G.; Staveley-O'Carroll, K. F.; Levitsky, H. I.; August, J. T.; Pardoll, D. M.; Wu, T. C. Treatment of Established Tumors with a Novel Vaccine that Enhances Major Histocompatibility Class II Presentation of Tumor Antigen. *Cancer Res.* **1996**, *56*, 21−26.
(44) Kerbel, R. S.; Kamen, B. A. The Anti-angiogenic Basis of Metronomic Chemotherapy. *Nat. Rev. Cancer* **2004**, *4*, 423−436.
(45) Fichorova, R. N.; Rheinwald, J. G.; Anderson, D. J. Generation of Papillomavirus-Immortalized Cell Lines from Normal Human Ectocervical, Endocervical, and Vaginal Epithelium that Maintain Expression of Tissue-Specific Differentiation Proteins. *Biol. Reprod.* **1997**, *57*, 847−855.
(46) Kenemans, P.; Davina, J.; De Haan, R.; Van Der Zanden, P.; Vooys, G.; Stadhouders, A. Surface Ultrastructure of the Uterine Cervix and Early Detection of Irreversible Neoplasia. In *Carcinoma of the Cervix*; Springer: New York, 1982; pp 91−99.
(47) Dawson, P. A.; Filipe, M. An Ultrastructural and Histochemical Study of the Mucous Membrane Adjacent to and Remote from Carcinoma of the Colon. *Cancer* **1976**, *37*, 2388−2398.
(48) Yin, G.-Y.; Zhang, W. N.; Shen, X.-J.; Chen, Y.; He, X.-F. Ultrastructure and Molecular Biological Changes of Chronic Gastritis, Gastric Cancer and Gastric Precancerous Lesions: a Comparative Study. *World J. Gastroenterol.* **2003**, *9*, 851−857.
(49) Thornton, J. M.; Todd, A. E.; Milburn, D.; Borkakoti, N.; Orengo, C. A. From Structure to Function: Approaches and Limitations. *Nat. Struct. Mol. Biol.* **2000**, *7*, 991−994.

DOI: 10.1021/am5016827
ACS Appl. Mater. Interfaces 2015, 7, 8961−8967